Journal of Energy Chemistry 27 (2018) 1292–1303

Contents lists available at ScienceDirect

Journal of Energy Chemistry

journal homepage: www.elsevier.com/locate/jechem

http://www.journals.elsevier.com/journal-of-energy-chemistry/

Review

Progress on the electrode materials towards vanadium flow batteries (VFBs) with improved power density

Tao Liu[a], Xianfeng Li[a,b,*], Huamin Zhang[a,b,*], Jizhong Chen[c]

[a] Division of Energy Storage, Dalian Institute of Chemical Physics, Chinese Academy of Sciences, Dalian 116023, Liaoning, China
[b] Collaborative Innovation Center of Chemistry for Energy Materials (iChEM), Dalian 116023, Liaoning, China
[c] State Key Laboratory of Operation and Control of Renewable Energy & Storage Systems, China Electric Power Research Institute, Beijing 100192, China

ARTICLE INFO

Article history:
Received 5 February 2018
Revised 4 July 2018
Accepted 5 July 2018
Available online 7 July 2018

Keywords:
Vanadium flow batteries
Polarization
Electrode
Carbon
Electrocatalyst

ABSTRACT

The vanadium flow battery (VFB) has been considered as one of the most promising large-scale energy storage technologies in terms of its design flexibility, long cycle life, high efficiency and high safety. However, the high cost prevents the VFB technology from broader market penetration. Improving the power density of the VFB is an effective solution to reduce its cost due to the reduced material consumption and stack size. Electrode, as one of the main components in the VFB, providing the reactions sites for redox couples, has an important effect on the voltage loss of the VFB associated with electrochemical polarization, ohmic polarization and concentration polarization. Extensive research has been carried out on the electrode modification to reduce polarizations and hence improve the power density of the VFB. In this review, state-of-the-art of various modification methods on the VFB electrode materials is overviewed and summarized, and the future research directions helpful to reduce polarization loss are presented.

Dr. Tao Liu received his Ph.D. in Materials Physics and Chemistry from Beihang University in 2010. Now he is an associate professor in Dalian Institute of Chemical Physics (DICP), Chinese Academy of Science. His research interests include electrode and bipolar plate or current collector materials for secondary battery applications (flow battery, lithium ion battery, etc.). Up to now, he is the author of more than 20 peer-reviewed papers and has applied more than 30 patents in battery field. He has received outstanding Science and Technology Achievement Prize of the Chinese Academy of Sciences.

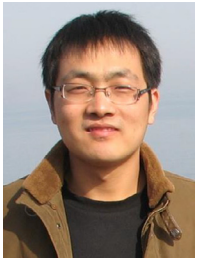

Dr. Xianfeng Li received his Ph.D. in Polymer Chemistry and Physics from Jilin University in 2006. After 3 years' postdoc with Prof. Vankelecom from K.U. Leuven University, he was appointed as associate professor in Dalian Institute of Chemical Physics (DICP), Chinese Academy of Science. In 2012, he was promoted as full professor. He currently serves as head of energy storage division at DICP. His research interests include functional membranes for secondary battery applications (Flow battery, lithium ion battery, lithium sulfur battery, etc.). Up to now, he is the author of more than 150 peer-reviewed papers with more than 4000 citations, his H-index is 36 and he applied more than 150 patents in battery field. He has received several awards from Chinese Government, including outstanding Science and Technology Achievement Prize of the Chinese Academy of Sciences, National Technology Invention Award, etc. He currently serves as the editorial board of "Scientific Reports" and "Journal of Energy Chemistry".

Dr. Huamin Zhang currently serves as a full professor at Dalian Institute of Chemical Physics (DICP), Chinese Academy of Science (CAS); He is also CTO of Dalian Rongke Power Co., Ltd., director of the state key lab of flow battery for energy storage. He got his bachelor degree from department of chemistry, Shandong University in 1982. Afterwards, he received his MS and Ph.D. degree from Kyushu University in 1985 and 1988, respectively. After several years' work in SUD-CHEMIE Japan, Osaka Gas Inc., Japan, he joined in DICP as a full professor in 2000. His research interests include the topic of energy and energy storage, e.g., fuel cells, flow batteries and batteries with high specific energy density. Professor Zhang has co-authored more than 260 research papers published in refereed journals and more than 150 patents. He has received numerous awards from Chinese Government including outstanding Science and Technology Achievement Prize of the Chinese Academy of Sciences, National Technology Invention Award and Dalian Technology Invention Award etc.

* Corresponding authors at: Division of Energy Storage, Dalian Institute of Chemical Physics, Chinese Academy of Sciences, Dalian 116023, Liaoning, China.
E-mail addresses: lixianfeng@dicp.ac.cn (X. Li), zhanghm@dicp.ac.cn (H. Zhang).

https://doi.org/10.1016/j.jechem.2018.07.003
2095-4956/

Dr. Jizhong Chen received the M.S. in Sichuan University and the Ph.D. degree from Institute of Electrical Engineering of the Chinese Academy of Sciences in 2001 and 2007, respectively. In 2007, he joined China Electric Power Research Institute. Since 2017, he has been as professorate senior engineer. His research areas are the integration, application and evaluation of large-scale energy storage technology.

1. Introduction

The environmental problem and energy shortage issues induced by the consumption of fossil fuels are becoming more serious, and the wide application of renewable energy is an inevitable choice to achieve sustainable social and economic development. However, since renewable energy from sources such as wind and solar power is intermittent, energy storage systems are required to combine with renewable power sources as a smart grid to improve grid reliability and utilization of renewable energy. Among various energy storage technologies, redox flow batteries (RFBs) seem to be an ideal storage technology for wind and solar electricity because of their perfect combination of design flexibility, long cycle life, high efficiency and high safety [1–4].

VFBs, proposed by Skyllas-Kazacos Maria's group at UNSW Australia [5], have become the most promising technology among the current flow batteries, because the same element is used in both the anolyte and the catholyte, which can alleviate the cross contamination issue through the membrane compared to other flow batteries. The electrochemical reactions during charge and discharge are as following:

Positive electrode reaction:

$$VO^{2+} + H_2O - e^- \underset{\text{discharge}}{\overset{\text{charge}}{\rightleftarrows}} VO_2{}^+ + 2H^+, \quad \varphi^\theta = 1.004\ \text{V} \tag{1}$$

Negative electrode reaction:

$$V^{3+} + e^- \underset{\text{discharge}}{\overset{\text{charge}}{\rightleftarrows}} V^{2+}, \varphi^\theta = -0.255\ \text{V} \tag{2}$$

Cell reaction:

$$VO^{2+} + H_2O + V^{3+} \underset{\text{discharge}}{\overset{\text{charge}}{\rightleftarrows}} VO_2{}^+ + V^{2+} + 2H^+, \quad \varphi^\theta = 1.259\ \text{V} \tag{3}$$

As shown in Fig. 1, the active species-vanadium ions, dissolved in the electrolyte, are circulated between the electrodes and electrolyte tanks by pumps. During charging/discharging, V^{2+}/V^{3+} and $VO^{2+}/VO_2{}^+$ redox reactions take place in the surface of electrode materials.

In the past few decades, VFBs technology has achieved significant progress. Up to now, many VFBs commercial demonstration systems at multi-MW levels have been installed in China, Japan and USA. However, the high cost is still one of the major factors that prevent the VFBs technology from broader market penetration. Improving the power density of VFBs is an effective solution to reduce the installed cost of VFBs due to the reduced material consumption and stack size. However, the increase of power density, that is the increase of current density, in a VFB will increase the polarization loss, resulting in lower energy efficiency. Therefore, to maintain the acceptable energy efficiency, the key of improving the power density of VFBs is to minimize various polarization (electrochemical, ohmic and concentration polarization) of VFBs.

As one of the key components, the electrode in VFBs plays a role of providing the active sites for vanadium ions redox reactions and has an important effect on the three polarizations of VFBs [6]. The electrical conductivity and thickness of the electrode will largely affect the ohmic polarization of VFBs. The electrocatalytic activity and reversibility of the electrode for vanadium ions redox reactions determine the electrochemical polarization, and its pore structure and hydrophilicity have a significant impact on the concentration polarization. Therefore, an ideal electrode material for VFBs should possess high electrical conductivity, electrocatalytic activity and reversibility, hydrophilicity and appropriate pore structure to reduce various polarizations of VFBs. In addition, the excellent chemical and electrochemical stability to ensure long cycle life and reasonable cost are also inevitable for the electrode materials of VFBs.

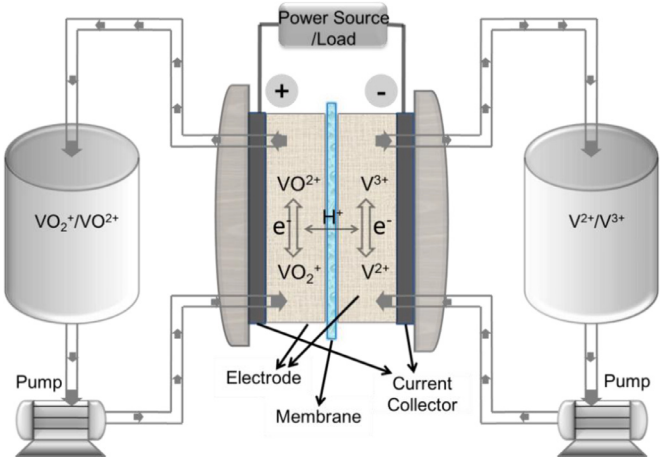

Fig. 1. Schematic representation of a VFB.

Although some review articles on VFB technology and electrode materials have been published [7–10], they put an emphasis on the technical trends in the electrode material selection and modification on the improvement of electrocatalytic activity. An insightful review, in terms of the effect of electrode modification on various polarization (electrochemical, ohmic and concentration polarization) of VFBs, has not been reported. Furthermore, the current state-of-the-art on the electrode materials in the recent years also need an update. In this review, state-of-the-art of various modification methods on the VFB electrode materials is overviewed and summarized according to their contribution to the three polarizations. Finally, the future research directions of high power density VFB electrode materials helpful to reduce polarization loss will be provided shortly.

2. Screen of electrode materials of VFBs

Skyllas-Kazacos Maria's group [11] initially investigated metal electrode materials such as Pb, Au, Pt, platinised titanium (Pt–Ti) and iridium oxide dimensionally stable electrodes (DSAs), and they found that Pb and Ti electrodes were easily passivated in the potential range of $VO^{2+}/VO_2{}^+$ redox reaction, Au electrode showed relatively poor electrochemical reversibility for the $VO^{2+}/VO_2{}^+$ redox reaction, and only DSAs electrode exhibited good electrochemical activity towards the $VO^{2+}/VO_2{}^+$ reaction without the problem of passivation film. However, DSAs electrode was excluded due to the problems of reduction of the iridium oxide coating in the potential range of V^{2+}/V^{3+} reaction and the high cost. After that, carbon materials, especially carbon fiber materials, attract their attention for the wide operation potential range, high chemical stability and reasonable cost. They compared two typical graphite felts based on rayon and polyacrylonitrile (PAN) precursors and found that various factors such as surface functional groups, electrical conductivity, surface area, microstructure and precursor materials affected their electrochemical performance [12]. PAN-based felt exhibited the superior electrochemical performance due to the

higher electrical conductivity and more resistance to oxidation. Thus PAN based carbon fiber materials such as carbon felt (CF) and graphite felt (GF) became the first choice of electrode material for VFBs due to their three-dimensional network structure, large specific surface area, as well as high conductivity, until now.

After entering 21th century, with the renewable energy rising, VFBs, as a promising candidate for the large scale EES, attract more researchers into this field. A large range of modification methods based on CF or GF electrode materials have been investigated. Nevertheless, most of studies have been focused on enhancing electrocatalytic activity of the electrode and lowering activation over-potential in this period.

In the recent years, to improve the power density of VFBs, electrode modification related to reducing ohmic polarization and concentration polarization was investigated as well, for example, reducing the thickness of the electrode, designing the hierarchical pore structure. These specific advances will be reviewed in more detail below.

3. Modification of electrode materials

As mentioned above, physicochemical properties of electrode material have a significant influence on the electrochemical performance. To reduce the polarization of VFBs, various modification methods on the electrodes have been investigated. This review clarified them according to their effect on the various polarizations.

3.1. To reduce electrochemical polarization of VFBs

Although carbon based electrode materials themselves have some catalytic activity, the modification of the electrode materials is necessary to improve the electrocatalytic activity and electrochemical reversibility, especially for VFBs operated at the higher current density. A variety of modification methods, such as introduction of surface functional groups, optimization of microstructure, increase of active surface area and introduction of electrocatalyst, have been carried out, and their effectiveness on the improving electrochemical activity of vanadium ions redox reactions has been validated.

3.1.1. Introduction of surface functional groups

As the earliest proposed modified strategy, the electrocatalytic effect of oxygen functional groups has been validated by Skyllas-Kazacos's group in the early 1990s [13,14]. They introduced oxygen functional groups onto the surface of graphite felt by thermal or acid treatment. Compared with the pristine graphite felt, significant improvement in electrocatalytic activity and energy efficiencies of VFB single cells were observed for the thermal or acid treated graphite felt. The increased electrocatalytic activity of the treated graphite felt was attributed to the increased amounts of oxygen functional groups like C–OH and C=O on the surface of carbon fiber. After that, various surface modification methods, such as electrochemical oxidation [15,16], wet-chemical treatment [17,18], plasma treatment [19–21], gamma irradiation [21], corona discharge [22], modified Hummers method [23], microwave treatment [24], have also been investigated, and the electrochemical performance of the treated carbon materials was improved due to the introduction of oxygen functional groups. Among these methods, plasma and microwave treatment methods are thought to be promising ones for the electrode materials of VFBs due to their environmental friendly, economic, and highly effective features.

Although oxygen functional groups can improve the hydrophilicity of carbonaceous surface and behave as the active sites for the vanadium ions redox reactions, overoxidation will reduce the electrical conductivity and strength of carbon electrode materials, and hence cause a decrease of electrochemical performance for VFBs. Di Blasi et al. [25] investigated the effect of the content of oxygen functional groups on the electrochemical performance of several graphite based electrodes, and found that an oxygen species content of about 4%–5% exhibited good electrochemical performance and an appropriate electrical conduction. Higher amount of oxygen functional groups led to an increase of the ohmic and charge transfer resistance then to a decrease of the electrochemical performance.

The influence of types of oxygen functional groups on the electrochemical performance is also a major concern of researchers in order to introduce the specific groups with the highest activity to reduce electrochemical polarization of VFBs. C–O, C=O and O–C=O groups are usually thought to be able to improve the electrocatalytic activity of the carbon electrode materials. While Estevez et al. [26], recently, tuned the type of oxygen functional groups on graphite felt electrodes by varying the oxidative techniques, and allowed for the direct comparison of the effect of specific oxygen groups on the electrochemical performance of the VFB cell. They found that O–C=O groups can facilitate the vanadium redox reaction and improve the VFB cells performance whereas the C–O and C=O groups degrade it. Nevertheless, such conclusions still need to be verified in other carbon materials.

For avoiding the negative effect of O groups on the electrical conductivity of carbon materials, nitrogen doping was paid attention since the five valence electrons of nitrogen atoms could contribute the extra charge to the bond in graphene layers, which enhances the electrical conductivity of nitrogen-doped carbon [27]. Furthermore, the high negative charge density of the incorporated nitrogen due to its strong electronegativity could facilitate the adsorption and coordination of vanadium ions on negatively charged nitrogen atoms [28], which results in a high electrocatalytic activity. Shao et al. [27] firstly investigated the electrochemical performance of nitrogen-doped mesoporous carbon materials (N-MPC), which is prepared by heat-treating mesoporous carbon in NH_3 for VFBs. The electrocatalytic kinetics and the reversibility of the redox couple VO^{2+}/VO_2^+ were significantly enhanced on N-MPC electrode compared with MPC and graphite electrodes. Other researchers [29–32] employed hydrothermal method to introduce N groups to carbon materials such as GF, carbon paper or carbon cloth, and found that these modified electrodes exhibited the improved hydrophilicity and electrochemical performance in VFBs.

It should be noted that, not the nitrogen doping level but the nitrogen type in the carbon materials determines the catalytic activity [28]. Among four types of nitrogenous groups, including pyridinic-N, pyrrolic-N, quaternary-N and oxidic-N, oxidic-N can be converted to pyridinic-N in an acidic environment, and nitrogen in pyridinic-N and pyrrolic-N configurations bears a higher negative charge density than quaternary nitrogen, which is more favorable for the adsorption of positively charged ions in solutions. However, the protonation reaction of these three nitrogen species in an acidic environment may make them inactive for vanadium ions redox reaction (Fig. 2(a)). While the quaternary nitrogen is more stable in an acidic environment since it is less susceptible to protonization. Therefore, the quaternary nitrogen can behave as active sites for the vanadium ions redox reaction. Jin et al. [28] proposed a mechanism of nitrogen-doped graphene (NGS) for the VO^{2+}/VO_2^+ redox reaction, as shown in Fig. 2(b). The possible formation of an N–V transitional bonding state, which facilitates the charge transfer between the electrode and vanadium ions, was thought to be a key step for its high electrocatalytic activity.

Apart from O and N functional groups, doping of P [33] also demonstrated the improved electrocatalytic activity. In the recent years, the co-doping of multi heteroatoms [34–40] was attempted to further improve the electrocatalytic activity of carbon electrode

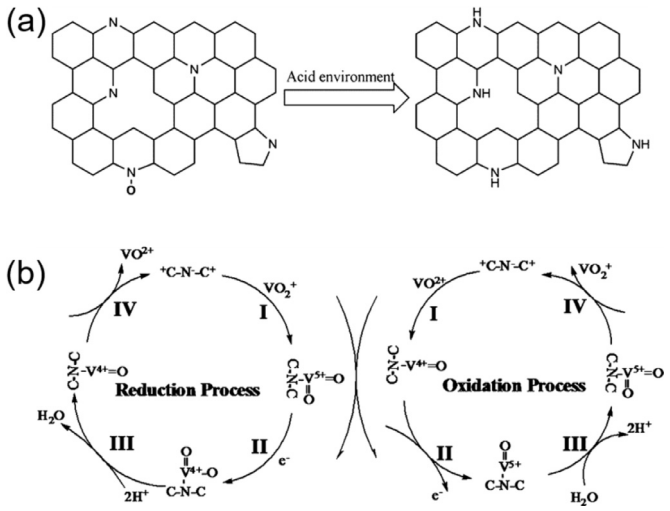

Fig. 2. (a) Protonation reaction of different nitrogen species in an acidic environment, (b) proposed catalytic mechanism of NGS for the VO^{2+}/VO_2^+ redox reaction [28].

materials. Lee et al. [35] treated graphite felt by thermal oxidation under air followed by thermal annealing with melamine as the nitrogen source. They found that the oxygen functional groups facilitate nitrogen doping in the carbon framework. A higher nitrogen content and pyridinic-N are observed when nitrogen is doped on the oxidized graphite surface using melamine compared to that of pristine graphite felt. As a result, the treated graphite felt (GFO + N) exhibits the higher electrocatalytic activity compared with GFO and GFN in VFBs (Fig. 3(a)). It exhibits a VE of 77.0% at a current density of 150 mA/cm^2 while VEs of pristine graphite felt and oxidized graphite felt are only 62.8% and 73.2%, respectively (Fig. 3(b)). In addition, co-doping of N/S [38] and B/N [40] in carbon structures has also been investigated, and the higher electrochemical performance ascribed to the synergistic effect of the heteroatoms compared with pristine carbon electrode or N-doped carbon has been demonstrated.

3.1.2. Optimization of microstructure

It is well known that the structure of PAN-based carbon fibers can be described by interlinked turbostratic layers with layer spacings significantly larger than graphite and rather small crystalline domains. Compared with basal plane, the edge plane sites of graphite exhibit the higher electrocatalytic activity towards V^{2+}/V^{3+} and VO^{2+}/VO_2^+ reactions because the increase of edge sites leads to a higher density of states at the Fermi level and thereby reduces an electrode-sided reaction limitation [41–44]. Pour et al. [45] proved that edge carbon sites provide faster kinetics for V^{2+}/V^{3+} and VO^{2+}/VO_2^+ redox reaction than basal carbon, especially at low vanadium concentrations, through cyclic voltammetry and symmetric flow cell measurements on selectively masked graphite foil and highly oriented pyrolytic graphite electrodes. As shown in Fig. 4, edge-exposed electrodes (blue) had more symmetric oxidation and reduction peaks, with small voltage separation between oxidation and reduction peaks, while basal-exposed electrodes (red) exhibited greater peak separation and more asymmetric oxidation and reduction currents for both V^{2+}/V^{3+} and VO^{2+}/VO_2^+ redox in comparison to unmasked graphite foil electrodes. The onset currents of oxidation peaks were shifted to lower voltages, while those of reduction peaks were shifted to high voltages for the edge-exposed electrodes in comparison to unmasked and basal-exposed electrodes. The unmasked electrodes were found to have combined responses from top-exposed and edge-exposed electrodes. Therefore, increase the ratio of edge-plane to exposed surface is beneficial to improve the electrocatalytic activity of carbon fiber based electrode materials.

To form more edge-plane sites, Maruyama et al. [46] carried out fine etching of the graphitized carbon fiber surface by coating the surface with a metal-containing carbonaceous thin film and thermal oxidation. They found that the finely etched surface possessed substantially enriched edge planes and an enhanced activity for the positive and negative electrode reactions of the VFB. The flow cell test with the carbon fiber electrodes after the tuned etching showed a significant decrease in the overpotential and an increase in the efficiency as well as stable cycling performance.

3.1.3. Increase of active surface area

Increasing the surface area, especially electrochemically active surface area, of carbon electrode materials is an effective approach to reduce the electrochemical polarization. For the conventional carbon fiber-based electrode materials, the specific surface area is relatively low (0.1–1 m^2 g^{-1}) due to the large diameter of carbon fiber which is usually 10–20 μm. To enlarge the specific surface area of electrode materials, many groups [47–51] attempted to activate the carbon fiber based electrode materials by physical activation and chemical activation methods.

Liu et al. [47] fabricated a kind of carbon paper (CP) with superhigh electrocatalytic activity via a universal and simple CO_2 activation method, as shown in Fig. 5. After activation, a large amount of macropores at several hundreds of nanometers level are evenly distributed on the surface of carbon fibers, and hence the BET specific surface area of CP increased dozens of times. Furthermore, the amounts of carbon edge atoms (defective carbon) and –OH group also increased. Therefore, the charge transfer resistance of a VFB with CP electrode after CO_2 activation decreased dramatically from 970 to 120 mΩ cm^2. Accordingly, the energy efficiency of a VFB with activated carbon paper as the electrode increased by 13% as compared to one without activation and reaches nearly 80% when the current density is 140 mA cm^{-2}.

Apart from CO_2, other activation agents such as steam [49], KOH [50–53], NiO [54] were also used to activate carbon fiber based electrode materials, and apparent improvement on the elecrocatalytic activity was observed. Compared with chemical activation, physical activation on the carbon fiber based materials is a simple, environmental friendly, time-efficient and potentially cost-effective activation method for commercial production because it does not need any chemical salts and time-consuming processing steps.

3.1.4. Introduction of electrocatalyst

Carbon based electrocatalyst: Similar to forming pores on the surface of carbon fiber by activation, addition of carbon-based material with high specific surface area on the supporting electrode also can increase overall electrode surface area. Therefore, a large amount of carbon nano materials such as carbon nanoparticles [55,56], carbon nanotube (CNT) [57–63], carbon nanofiber (CNF) [64–67], graphite oxide [68,69], graphene oxide (GO) nanosheet [70,71], thermal reduced graphite/graphene oxide [69,72–74], have attracted many researchers' attention due to their high specific surface area, electrical conductivity and stability in acid media. And all of them demonstrated the high electrocatalytic activity toward vanadium ion redox reactions, especially functionalized carbon nano materials [28,60,75–78] and hybrid carbon nano materials such as graphene oxide nanosheets/multi-walled carbon nanotubes (GO/MWCNTs) [79,80], and carbon nanotubes/carbon nanofibers (CNTs/CNFs) [81]. For example, electrodes based on single GO nanosheets suffered from low rate capability because of their rather poor electrical conductivity, thus the energy efficiency and power capability were severely limited. Therefore, in order to improve the electron and ion transport capability, Han

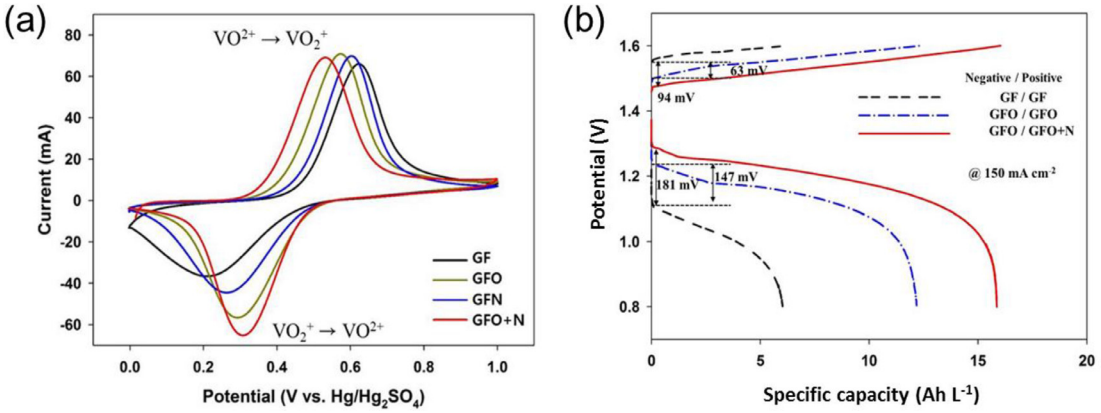

Fig. 3. (a) Cyclic voltammograms of GF, GFO, GFN and GFO+N electrodes in 0.1 M $VOSO_4$ + 3.0 M H_2SO_4 electrolyte at a scan rate of 5 mV s^{-1} with potential window of 0.0 V to 1.0 V vs. Hg/Hg_2SO_4, (b) charge–discharge curves of VFBs employing different graphite felts as negative and positive electrodes at a constant current density of 150 mA cm^{-2}. The upper voltage limit was set to 1.6 V for charging, and the lower voltage limit was set to 0.8 V for discharging [35].

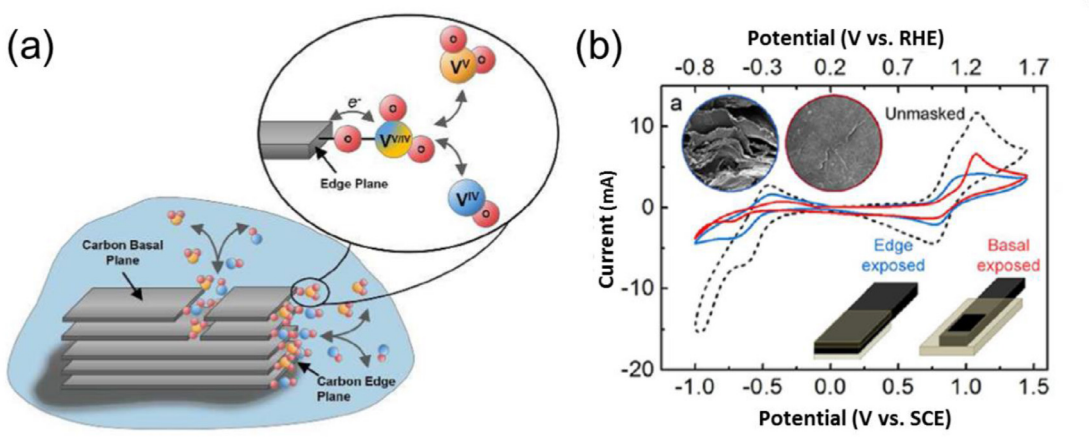

Fig. 4. (a) Schematic of carbon basal plane and edge plane, (b) steady-state CVs measured in 0.5 M VO^{2+} in 2 M H_2SO_4 electrolyte. Graphite foil (GF) electrodes: unmasked (dashed-black line), edge- (blue line), and basal-exposed (red line) GF electrodes with schematics and scanning He-ion microscope images in the insets. All CV were collected at a scan rate of 20 mV/s from a three-electrode cell setup, with graphite foil and SCE used as the counter and reference electrodes, respectively [45].

et al. [79] fabricated a GO nanosheets/multi-walled carbon nanotubes (GO/MWCNTs) hybrid on a glassy carbon electrode (GCE) by an electrostatic spray technique after efficient ultrasonic treatment. The results showed that GO nanosheets and MWCNTs form an electrocatalytic hybrid carrying a mixed conducting network after the introduction of MWCNTs. Compared with the pure GO nanosheets and MWCNTs, GO/MWCNTs hybrid exhibited a much better electrocatalytic redox reversibility towards VO^{2+}/VO_2^+ redox couples.

Regarding the loading methods of carbon based electrocatalyst on the supporting electrode, in the early stage, Li et al. [57,59] used dip-coating method to coat SWCNT or MWCNT on the surface of carbon felt and obtained improved VE and EE at the current density of 20 mA cm^{-2}. However, the major disadvantage associated with this method is the fact that attachment between the high-surface-area materials and the carbon fiber surfaces relies on weak Van der Waals forces. Flowing electrolyte can easily destroy or disrupt the attachment, causing a severe problem in durability.

Afterward, several groups have reported to synthesize CNTs, CNFs or graphene directly on the carbon fiber surfaces via chemical vapor deposition (CVD) processes, aiming to connect the high surface area material with carbon fiber surfaces via covalent bonds [67,81,82]. For instance, Park et al. [81] grew CNF/CNT composite catalysts on carbon felt (CF) through the thermal decomposition of acetylene gas over Ni catalysts (Fig. 6(a)). The electrode with the composite catalyst prepared at 700 °C (denoted as CNF/CNT-700) demonstrates the best electrocatalytic properties toward the V^{2+}/V^{3+} and VO^{2+}/VO_2^+ redox reactions. Moreover, this composite electrode in a VFB single cell exhibits improved energy efficiency by about 25% at 100 mA cm^{-2} compared to untreated CF electrode due to the enhanced surface defect sites of exposed edge plane in CNF and a fast electron transfer rate of in-plane side wall of the CNT. However, complex and tedious preparation process of CVD method hinder its mass production significantly.

To seek for a suitable for industrial production and economic deposition method, electrophoretic deposition [83] and passive deposition (also known as flowing deposition) [84,85] methods were reported recently for the VFB electrode preparation. Gonzalez et al. [83] prepared a graphene-modified graphite felt from a raw graphite felt and a graphene oxide water suspension by means of electrophoretic deposition (EPD). The remarkably enhanced electrocatalytic performance of the resultant hybrid material, in terms of electrochemical activity and kinetic reversibility towards the VO^{2+}/VO_2^+, and mainly the markedly high energy efficiency of the VFB single cell (ca. 95.8% at 25 mA cm^{-2}) can be achieved due to the 3D-architecture consisting of fibers interconnected by graphene-like sheets. Aaron et al. found that reduced graphene oxide (rGO) or Vulcan carbon black (XC-72R) can be passively deposited on the carbon felt supporting electrode by adding a suspension of rGO or XC-72R to the electrolyte reservoirs. Addition

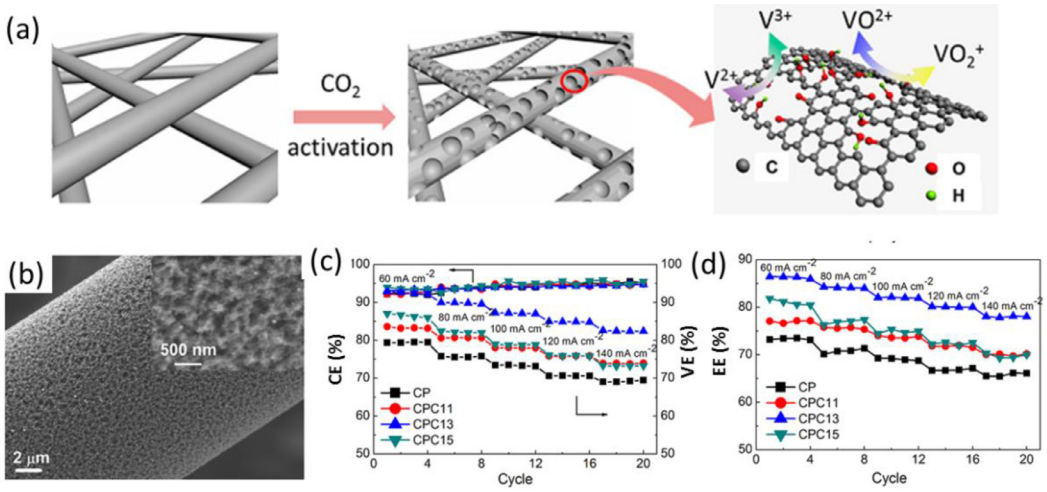

Fig. 5. (a) Schematic principle of electrode preparation, (b) SEM images of CP activated by CO_2 at 1300 °C; electrochemical performance of VFB single cells with CP as received and activated by CO_2 as electrodes, respectively: (c) CE and VE, (d) EE [47].

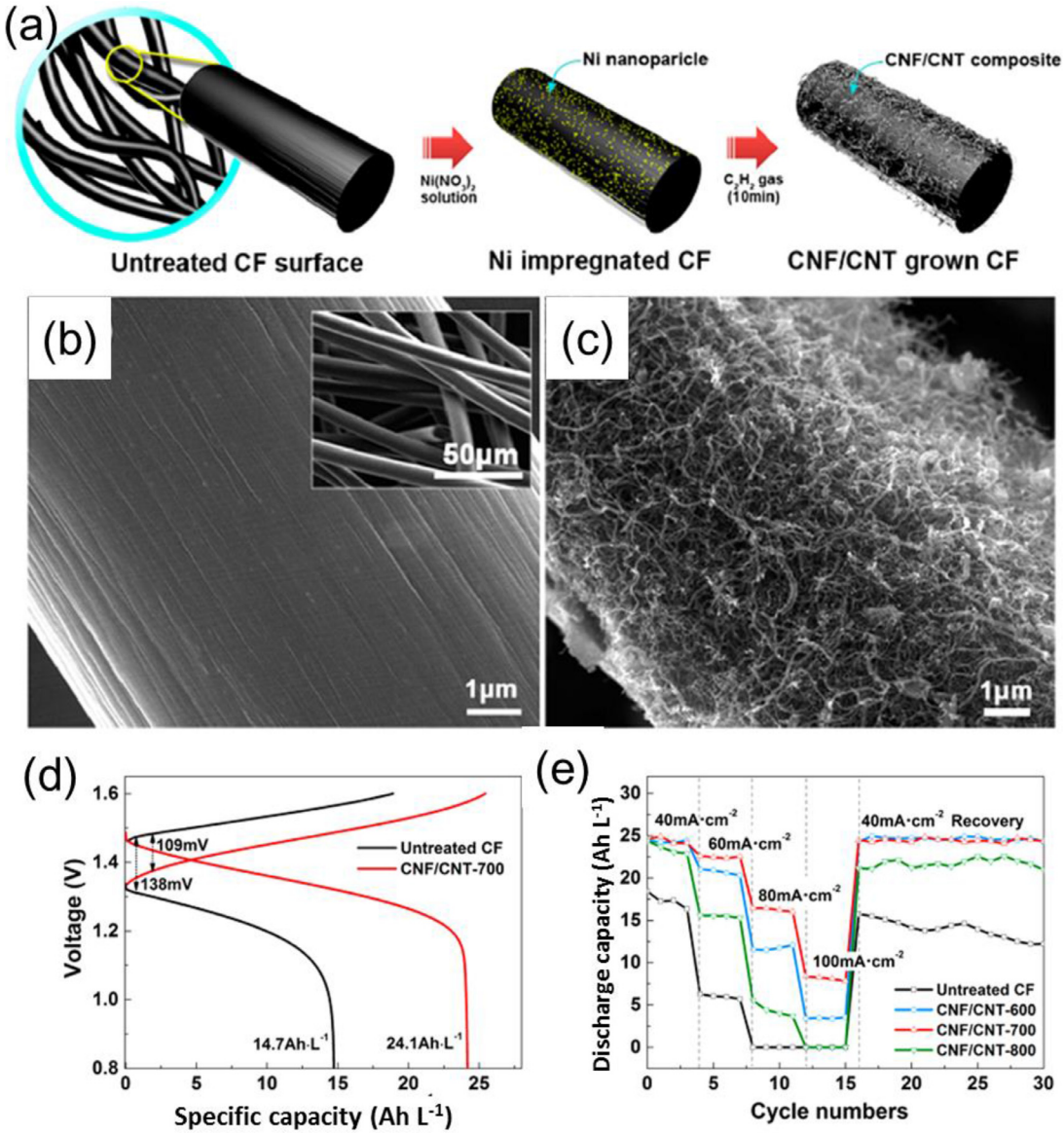

Fig. 6. (a) Schematic view for the synthesis of CNF/CNT grown on carbon felt surface on Ni nanoparticle seeds via C_2H_2 gas decomposition above 500 °C, SEM image of (b) untreated CF and (c) CNF/CNT grown CF surface prepared at 700 °C; Electrochemical performance of VFB employing CNF/CNT-T electrodes at room temperature: (d) charge–discharge voltage profiles of untreated and as-prepared electrode at 40 mA cm^{-2}, (e) rate performance with increasing the current rate from 40 to 100 mA cm^{-2} [81].

of rGO flakes or XC-72R enables a tripling of current density at the same 80% voltage efficiency compared with pristine carbon felt electrodes. Moreover, despite that the surface area enhancement ascribed to the addition of rGO or XC-72R is expected to partially wash out over time, the flowing deposition treatment could potentially be reapplied to recover optimal performance without opening the cell.

Metal based electrocatalyst: In the early 1990s, Skyllas-Kazacos's group [11] has investigated the electrochemical behavior of metallized graphite fiber electrode prepared by impregnation or ion-exchange with solutions containing Pt^{4+}, Pd^{2+}, Au^{4+}, Mn^{2+}, Te^{4+}, In^{3+} and Ir^{3+} in VFBs. The cyclic voltammetry results showed that electrodes modified by Pt^{4+}, Pd^{2+} and Au^{4+} are unsuitable due to the increased hydrogen evolution rates, while the electrodes treated with Mn^{2+}, Te^{4+}, In^{3+} and Ir^{3+} exhibited the significantly improved electrochemical activity compared with the untreated fiber electrode. Among of them, the electrode modified by Ir^{3+} exhibited the best electrochemical behavior for the various vanadium redox species. Afterward, Wang and Wang [86] studied the performance of the graphite felt modified by pyrolysis of Ir reduced from H_2IrCl_6. AC impedance and steady-state polarization measurements showed that the Ir-modified materials have improved activity and lowered overpotential of the desired VO^{2+}/VO_2^+ redox process. Furthermore, a decrease of 25% in cell resistance was observed for a cell with Ir-modification of graphite felt as the electrodes compared to the cell using non-modified felt due to the enhanced electro-conductivity.

Among various metal electrocatalysts, bismuth (Bi) has received the most attention due to its low cost, non-toxicity, and high hydrogen evolution overpotential [87–91]. Gonzalez et al. [87] firstly investigated the electrochemical behavior of a GF modified with thermally reduced bismuth as positive electrode in a VFB. Despite the low metal content (1 at%) on the surface of carbon fiber, the Bi modified GF showed an excellent electrocatalytic activity and stability for the VO^{2+}/VO_2^+ redox reaction. Therefore, they believed that bismuth nanoparticles on the carbon surface can act as stable active sites for the VO^{2+}/VO_2^+ redox reaction. After that, Li et al. [88] found that, as shown in Fig. 7, by employing electrolytes containing Bi^{3+}, bismuth nanoparticles can only be electrodeposited onto the surface of a graphite felt negative electrode during operation of a VFB and facilitate the redox reaction between V^{2+} and V^{3+}. Furthermore, Bi nanoparticles significantly improve the electrochemical performance of VFB single cells by enhancing the kinetics of the sluggish V^{2+}/V^{3+} redox reaction, especially under high power operation. The energy efficiency is increased by 11% at 150 mA cm^{-2} owing to faster charge transfer as compared with one without Bi, as shown in Fig. 7(d). In view that Bi nanoparticles cannot be electrodeposited on the surface of carbon fibers for the positive electrode CF during operation of the VFB, it cannot be concluded that Bi nanoparticles have no positive effect on the VO^{2+}/VO_2^+ redox reaction. Zhang's group [91] prepared Bi-modified CF by traditional high-temperature H_2 reduction method and investigated the effect of Bi nanoparticles for both VO^{2+}/VO_2^+ and V^{2+}/V^{3+} redox couples. Results showed that, due to the relatively low standard redox potential of Bi^{3+}/Bi redox couple, all of Bi was oxidized to Bi^{3+} with no electrochemical activity before VO^{2+} transforming into VO_2^+. Therefore, Bi has no electrocatalytic activity for VO^{2+}/VO_2^+ redox reaction and can only be used as the electrocatalyst for V^{2+}/V^{3+} redox reaction.

Transition metal oxides can be applied as electrocatalysts due to their abilities to change between their various valency states and to absorb reactive species as active center. It has been reported that PbO_2 [92], MoO_2 [93] and CeO_2 [94,95], can enhance the kinetic rate of VO^{2+}/VO_2^+ redox reaction, TiO_2 [96] can accelerate the V^{2+}/V^{3+} reaction, while WO_3 [97,98], ZrO_2 [99], Mn_3O_4 [100,101], and Nb_2O_5 [102] have been reported to improve the electrocatalytic activity towards vanadium ion redox reactions. Especially WO_3, ZrO_2, Mn_3O_4, and Nb_2O_5 can be used as the electrocatalysts for both positive and negative electrodes.

In the recent years, transition mental nitrides (TMN) and transition metal carbides (TMC) such as TiN [103–105] and TiC [106] attracted researchers' attention due to their remarkably higher electrical conductivity than transition metal oxides. Zhao's group [105] prepared a highly catalytic and stabilized titanium nitride (TiN) nanowire array-decorated graphite felt electrode for VFBs. TiN nanowires are synthesized by a two-step process, as shown in Fig. 8(a), in which TiO_2 nanowires are first grown onto the surface of carbon fiber via a seed-assisted hydrothermal method and then converted to TiN through nitridation reaction. The results showed that the rutile TiO_2 could be completely converted to cubic TiN after annealing in NH_3 at a temperature of 800 °C (Fig. 8(b)). The prepared TiN nanowire decorated graphite felt electrode enabled the energy efficiency of a VFB single cell to be 77.4% at a current density of 300 mA cm^{-2}, which is correspondingly 15.4% higher than that of single cell assembled with a pristine GF electrode (Fig. 8(c)). The superior performance is ascribed to the significant improvement in the electrochemical kinetics and enlarged active sites toward V^{2+}/V^{3+} redox reaction.

In addition, it should be noted that the exploitation of synergistic interactions between the electrocatalyst and electrocatalyst support is becoming a promising trend in electrocatalyst development. Such interactions result from the presence of dual active sites at the electrocatalyst/support interface [107–110]. Ejigu et al. [107] investigated electrocatalytic synergism in an N-doped rGO/Mn_3O_4 composite electrocatalyst for VO^{2+}/VO_2^+ electrochemistry. Electrochemical analysis shows that, as shown in Fig. 9, the electrocatalytic activity of the composite electrocatalyst is significantly higher than those of the individual components due to synergism between the Mn_3O_4 nanoparticles and the carbonaceous support material. Furthermore, electrocatalysis of the redox reaction is most effective when nitrogen is present within the support framework, demonstrating that the metal–nitrogen–carbon coupling is the key to obtain the high electrocatalytic activity for VO^{2+}/VO_2^+ redox reaction.

3.2. To reduce ohmic polarization of VFBs

Ohmic polarization of a VFB, that is the internal resistance of a VFB, consists of the resistance to ionic transport through the electrolyte and membrane, electrical resistance in the electrodes and bipolar plates, and contact resistance between cell components. The currently commercialized VFB usually adopts a flow-through structure, as shown in Fig. 10(a), in which the electrolyte is pumped through the porous electrode such as CF or GF via flow channels in the electrode frame. The resistance of the electrode and contact resistance of the bipolar plate and electrode largely depend on the electrode compression, and both of them decrease as the electrode compression increases [111–114]. Nevertheless, the increase of electrode compression also leads to a decrease of porosity of the electrode, which is detrimental to electrolyte transport. The trade-off between these two effects leads to an optimized compression ratio of 20% to achieve the highest energy efficiency [111].

Despite that, CF or GF electrode of conventional VFB with flow-through structure has to be relatively thick (3–6 mm), since the lay-out of the flow channels restricts the thickness of the electrode frame to be larger than 3 mm usually. As a result, the ohmic resistance of the VFB is still relatively high, which limits the VFB to an operating current density lower than 150 mA cm^{-2} under the premise of keeping EE not lower than 80%. It has been reported that the proportion of ohmic polarization of a VFB, employing CF or GF, accounting for about 64% of all the polarizations

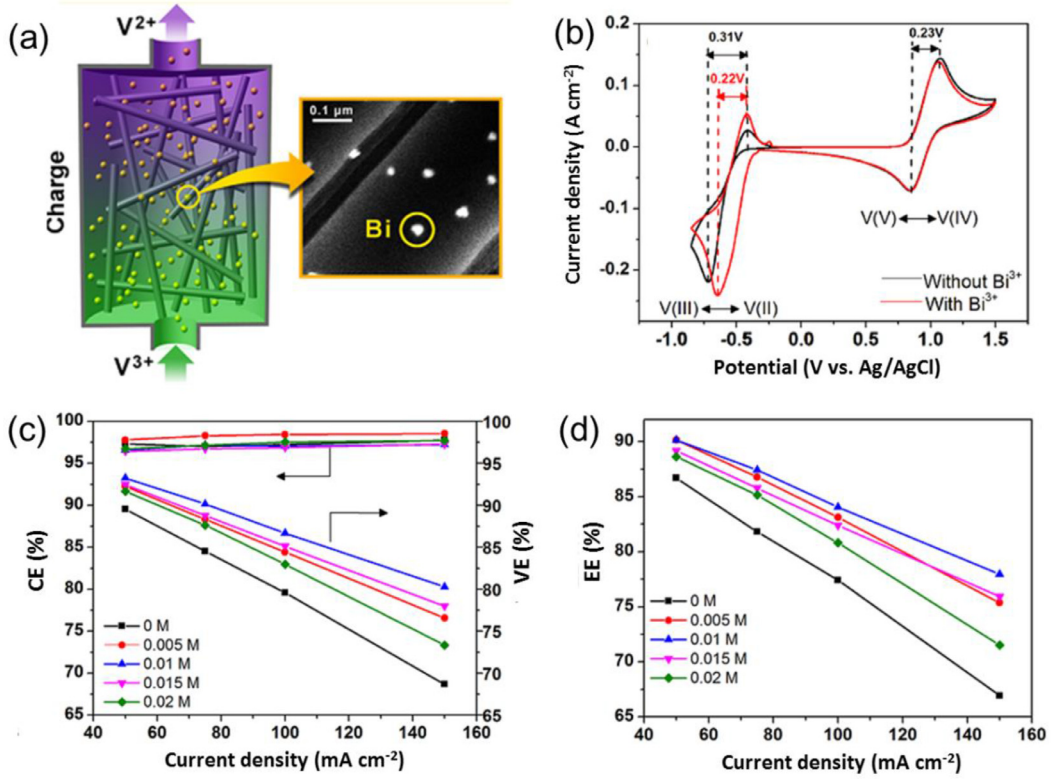

Fig. 7. (a) STEM image of Bi nanoparticles in the anolytes resulting after cycling, (b) cyclic voltammograms with glassy carbon as working electrode in solutions of 2 M $VOSO_4$ + 5 M HCl with or without 0.01 M $BiCl_3$ at a scan rate of 50 mV s^{-1}; Electrochemical performance of VFBs employing electrolytes containing different Bi^{3+} concentrations as a function of charge/discharge current density: (c) CE and VE, (d) EE [88].

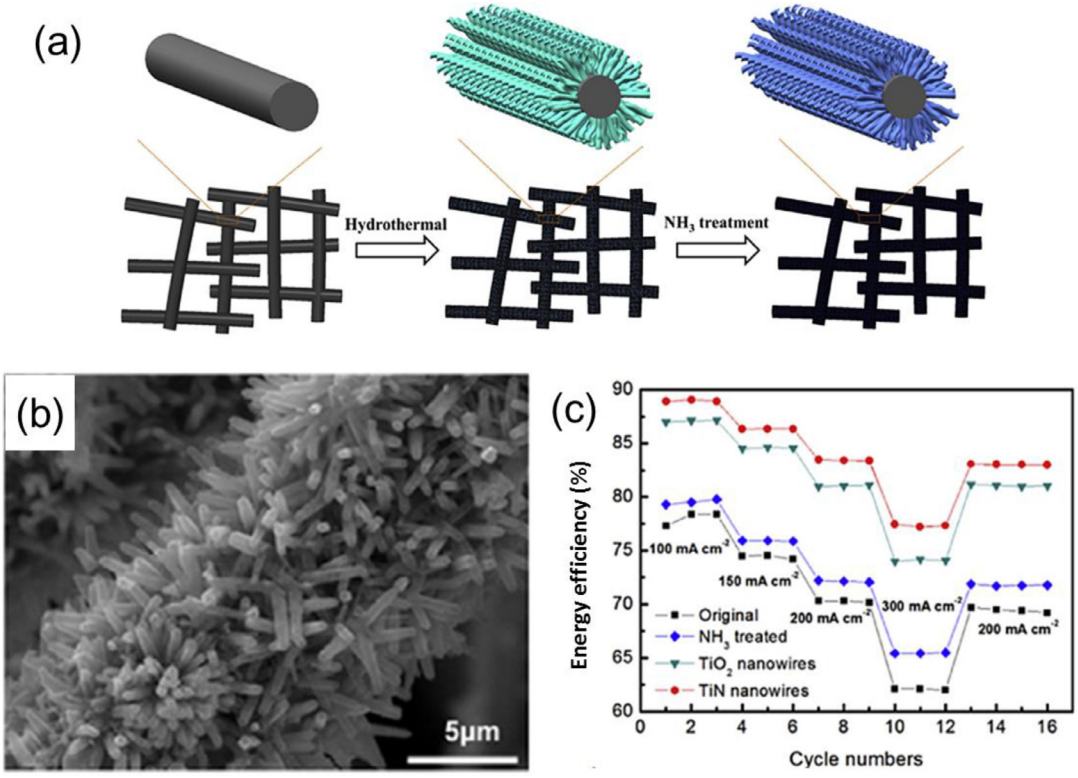

Fig. 8. (a) Schematic diagram of the two-step growth process for preparing TiN nanowires on the surface of graphite felt, (b) TiO_2 nanowires annealed in NH_3 at temperature of 800 °C, (c) energy efficiency as a function of cycle number at different current densities [105].

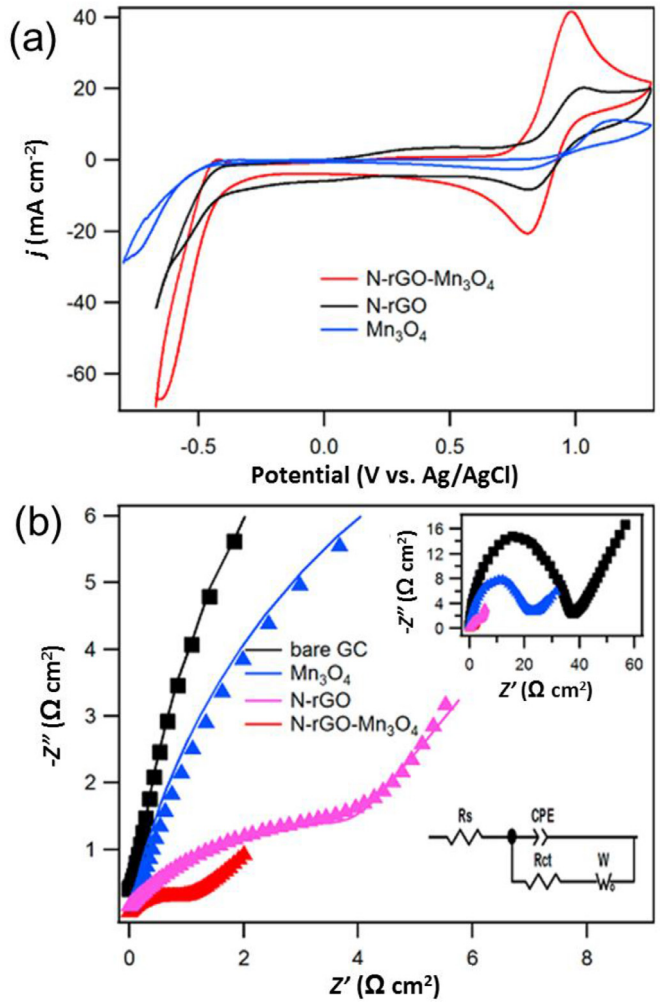

Fig. 9. (a) CVs recorded at N-rGO-Mn_3O_4-, N-rGO-, and Mn_3O_4-modified GC electrodes at 30 mV s^{-1} in 1.0 M $VOSO_4$/2.0 M H_2SO_4 by cycling the potential between −0.7 V (initial) and 1.3 V for both N-rGO-Mn_3O_4 and N-rGO, and between −0.9 V (initial potential) and 1.3 V for free Mn_3O_4. (b) Nyquist plots obtained using the electrodes indicated in panel A. The measurements were carried out at an amplitude of 5 mV in the frequency range from 100 mHz to 100 kHz and at an applied potential of 0.95 V. The main frame shows the high-frequency region of the plots shown in the upper right inset [107].

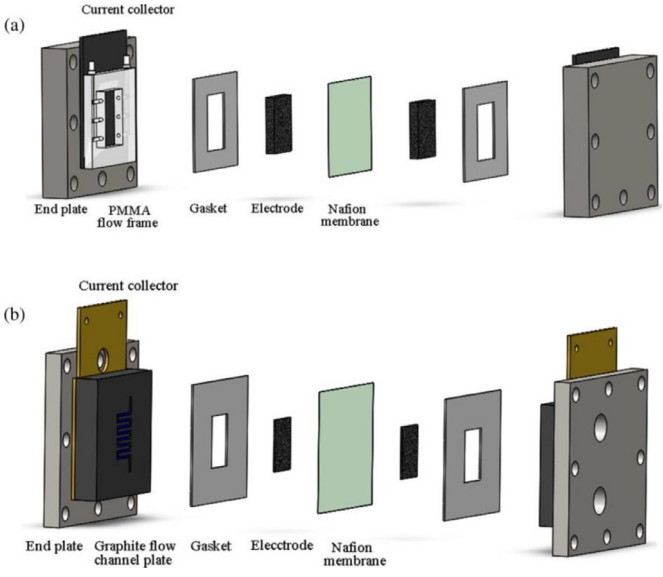

Fig. 10. Schematic of a VFB structure. (a) Flow-through structure without flow fields, (b) flow-by structure with single serpentine flow field [56].

[90]. Furthermore, because the ohmic overvoltage is proportional to the operating current, the ohmic loss can be expected to become more serious when operating at a high power/current region [115]. Therefore, to improve the power density of VFBs, the thickness of the electrode should be decreased as possible to reduce the ohmic polarization.

In this regard, some researchers [116–120] introduced the zero-gap structure used in the fuel cell into the VFB structure design. They replaced graphite felt electrodes to a thinner carbon paper or carbon cloth cooperating with the flow-by mode as shown in Fig. 10(b). This novel cell configuration, exhibiting a much smaller area specific resistance (ASR) of 500–600 mΩ cm^2, enables the VFB to achieve a significantly improved power density compared with conventional flow-through structure [117]. However, the reduction in the surface area of the electrode with the decrease of the electrode thickness, will lead to a large electrochemical polarization. Mench's group [117] found that stacking 3 layers thermally treated carbon paper together as the electrode, along with the use of Nafion 212 membrane, can obtain the highest peak power density of 767 mW cm^{-2}.

To minimize the ohmic polarization of the VFB, the thickness of the electrode was further reduced by Xu et al. [121] using the electrospun carbon nanofiber web (ECNFW) with the thickness of only 50 μm as the elelctrode independently. As expected, the ASR of the VFB single cell with ECNFW electrodes is only around 250 mΩ cm^2, which is almost a half of that of the VFB with carbon paper electrodes. However, the huge concentration polarization due to the small pore size in a VFB with ECNFW electrodes caused a significant decline of the charge/discharge performance (EE is only 74.1% at 40 mA cm^{-2}). Therefore, to improve the mass transfer ability of active species in ECNFW, the pore size of ECNFW was enlarged by blending electrospinning method, which will be descripted in the following section.

In short, reducing the thickness of the electrode will shorten both ion transport and electron transport distances, resulting in a decrease of the ohmic polarization. On the other hand, it will also reduce the surface area and the hydraulic permeability of the electrode, corresponding to an increase of the electrochemical polarization and concentration polarization. Therefore, it is necessary to determine the optimum electrode thickness for various electrode materials with the different electrocatalytic activities and pore structures by the trade-off among these three effects to achieve the best battery performance.

3.3. To reduce concentration polarization of VFBs

Insufficient mass transport of active species is also a main limiting factor in the development of the VFBs with high power density because the faster reaction rate requires more active species. It is well known that increasing flow rate of electrolyte can enhance the mass transport and decrease concentration polarization, but this method increases the energy consumption of pump simultaneously, hence lowering the overall energy efficiency of the VFB system. Therefore, to increase the electrode permeability by optimizing the porous structure, such as pore sizes, pore distributions and pore shapes, of the electrode is a better solution strategy [122–125].

For the conventional VFBs with flow-through structure, the concentration polarization is not large compared with other two polarizations due to the low flow resistance caused by the adoption of thick electrode material and high porosity of CF or GF (usually >90% under the compression of 20%). Even though, the use of suitable flow channels can improve flow distribution through the electrodes and reduce flow resistance, hence reducing the energy consumption of the pumps. Bhattarai et al. [124] compared four types of electrodes with different channels with a conventional electrode

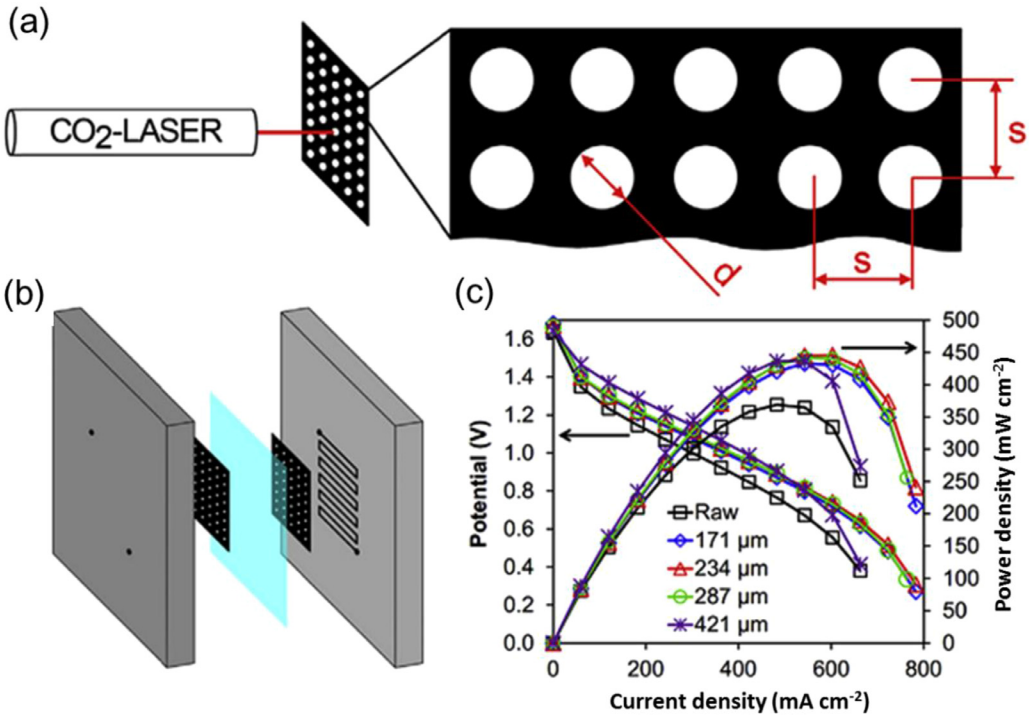

Fig. 11. (a) Schematic of the laser perforation process, (b) the flow cell setup with laser-perforated electrodes, (c) polarization curves for perforated electrodes with varying pore sizes [123].

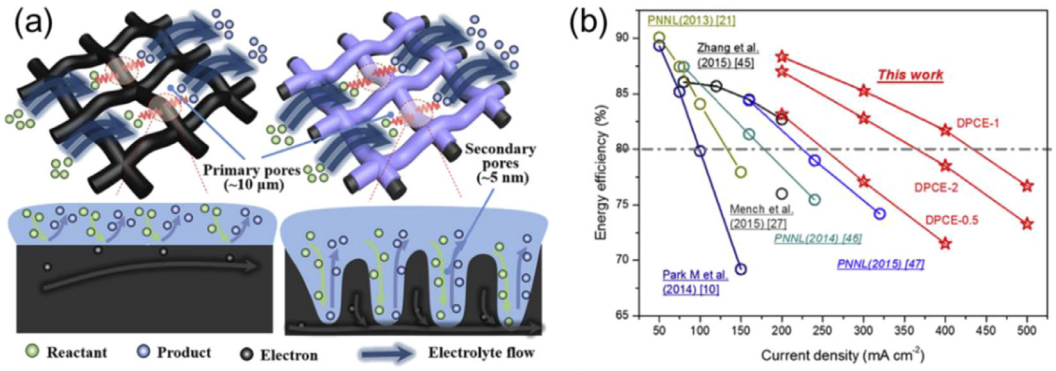

Fig. 12. (a) The schematic of the conventional carbon-fiber based electrode and the proposed dual-scale porous carbon electrode, (b) the comparison of the performance of VFBs with DPCE-0.5/1/2 and those in the open literature [120].

without channels and found that the overall energy efficiency increased by 2.7% at 80 mA cm^{-2} by the adopt of interdigitated open channels due to the improvement in flow distribution and pump power reduction. Nevertheless, the CNC machining channels on the felt electrode material are not suitable for the large-scale production in terms of the difficult processing and economy.

While for the VFBs with zero-gap structure, the concentration polarization becomes relatively apparent due to the adoption of thin electrode material such as carbon paper or carbon cloth and their low porosity of about 80%. To improve the electrolyte accessibility, Mayrhuber et al. [123] created macro-scale pores of different sizes and distributions in the carbon paper electrode as the transport channels by a CO_2 laser-perforation method, as shown in Fig. 11. Such macropores provided a more facile route for electrolyte to enter and permeate through the electrode, thus improve the supply of reactants to the active surface area of the material, and obtained a 30% increase in peak power density for the laser perforated electrode with 234 mm diameter holes and 352.8 holes cm^{-2} compared to the raw unperforated electrode.

However, excessive perforation of the carbon paper electrode will lead to a reduced active surface area, which causes a larger activation loss and limits the increase in cell performance. To resolve such conflict, Zhao's group [120] prepared a dual-scale porous carbon electrode (DPCE) by KOH activation of carbon paper, which possesses two types of pores: the large pores (~10 μm) formed between carbon fibers serve as the transport pathways for electrolyte, while the small pores (~5 nm) formed on carbon fiber surfaces act as active sites for rapid electrochemical reactions, as shown in Fig. 12(a). The battery with the optimum DPCE exhibited the EE of 82% at the current density of 400 mA cm^{-2}, which is the highest cell performance reported to date (Fig. 12(b)).

Recently, a novel method to fabricate the large pores electrode materials was reported by Xu et al. [125]. They prepared a free-standing carbon nanofiber web with large pores through the horizontally-opposed blending electrospinning of PAN and polyvinyl pyrrolidone (PVP) and the following removal of PVP fiber. With the employment of such electrode material, the concentration polarization of the VFB was effectively reduced due to the

larger pore size and higher porosity, and the VE obtained an increase over 10% at 60 mA cm^{-2}.

4. Conclusions and perspective

The vanadium flow battery (VFB) has been considered as one of the most promising large-scale energy storage technologies in terms of its design flexibility, long cycle life, high efficiency and high safety. However, the high cost prevents the VFB technology from broader commercialization. Improving the power density of the VFB is an effective solution to reduce its cost due to the reduced material consumption and stack size. Various electrode modification researches have been carried out to reduce polarization loss and improve the power density of the VFB.

Up to date, most study focused on improving the electrocatalytic activity of the electrode materials to reduce the electrochemical polarization, by introducing surface functional groups, optimizing the microstructure of carbon materials, enlarging the surface area and loading electrocatalysts. O groups can improve the hydrophilicity and electrocatalytic activity of carbon materials in the VFB, but reduce their electrical conductivity. Thus the trade-off of these two effects needs to be considered. It is attractive for N groups since they can simultaneously improve the hydrophilicity and electrocatalytic activity, as well as the electrical conductivity. Nevertheless, the more efficient and environmental-friendly N-doping method is necessary for industrial production. Increasing the edge carbon sites in the carbon electrode, enlarging the electrochemical active surface area by forming pores on the carbon fiber surface or loading carbon nanomaterials with high surface area, and introducing high efficient metal-based electrocatalysts can all improve the electrocatalytic activity of carbon electrode materials and obtain the higher battery performance. Furthermore, the synergistic effect of multi functional groups or various modification methods has been preliminarily demonstrated to obtain the higher electrocatalytic performance compared with only one functional group or modification method. In the future study, it is necessary to further study the synergistic effect between multi functional groups, or electrocatalyst and supporting materials, or various modification methods, on the carbon electrode materials, and find a more optimized combination to further improve the electrochemical performance of the electrode. In addition, the study on the negative electrode reaction should be emphasized because more and more reports showed that the performance of a VFB is limited by the poor reaction kinetics and high activation losses in the negative half-cell.

Thin electrode has become the development trend of electrode for VFBs with higher power density because it can reduce the ohmic polarization of VFBs to a large degree. However, it simultaneously reduces the actual surface area per apparent surface area and increase flow resistance, leading to increased electrochemical and concentration polarizations. Therefore, the electrode material with the higher electrocatalytic activity and proper pore structure need to be developed. In addition, the employment of zero-gap structure must collocate with the bipolar plate with flow field. At present, graphite plate with flow field was usually used as the bipolar plate in the open reports. However, the brittle nature and high cost restrict its industrial application. Therefore, the development of carbon plastic composite bipolar plate with high electrical conductivity is the key of the industrial application of such structure.

For the concentration polarization, less attention was paid on the reduce of the concentration polarization of VFBs since the concentration polarization of VFBs with CF or GF as the electrodes is not large. With the thickness of electrode decreases, the flow resistance increases, accordingly concentration polarization increases. Except designing the flow channels on the surface of bipolar plate, optimizing the porous structure, such as pore sizes, pore distributions and pore shapes, of the electrode to increase the electrode permeability is a better solution strategy. Especially the designing of hierarchical pore structure, can effectively resolve the issues, including high flow resistance, low porosity and active surface area, that caused by the thin electrode. In the following study, the optimization of pore size of hierarchical pore, including the large pores serve as the transport pathways for electrolyte and small pores act as active sites for redox reactions, is essential to further reduce the concentration polarization.

In addition, to provide the guideline for the design of the high-performance electrode material for VFBs, fundamental studies on the electrocatalytic mechanism of various functional groups and electrocatalysts toward vanadium ion redox reactions should be pursued. More investigations and assessments had better be performed according to the unified standard, including preparation of working electrode, assembling of battery and test condition, to make the electrochemical performance data obtained by various research groups comparable.

In general, it is promising to develop the high-performance electrode material, which is easy for industrial production, to improve the power density of VFBs and to make VFBs more commercially competitive.

Acknowledgments

This work was supported by the National Natural Science Foundation of China (Grant no. 21506210), the Outstanding Young Scientist Foundation, Chinese Academy of Sciences (CAS) and State Grid Corporation of Science and Technology Projects (Research on key technology of bipolar plate material development and engineering for vanadium redox flow battery).

References

[1] A.Z. Weber, M.M. Mench, J.P. Meyers, P.N. Ross, J.T. Gostick, Q. Liu, J. Appl. Electrochem. 41 (2011) 1137–1164.
[2] G.L. Soloveichik, Battery technologies for large-scale stationary energy storage, in: J.M. Prausnitz (Ed.), Annual Review of Chemical and Biomolecular Engineering, 2, 2011, pp. 503–527.
[3] G. Kear, A.A. Shah, F.C. Walsh, Int. J. Energy Res. 36 (2012) 1105–1120.
[4] H. Zhang, X. Li, J. Zhang, Redox Flow Batteries: Fundamentals and Applications, CRC Press, Taylor &Francis Group, New York, 2017.
[5] M. Skyllas-Kazacos, M. Rychcik, R.G. Robins, A.G. Fane, M.A. Green, J. Electrochem. Soc. 133 (1986) 1057–1058.
[6] C. Ding, H. Zhang, X. Li, T. Liu, F. Xing, J. Phys. Chem. Lett. 4 (2013) 1281–1294.
[7] A. Parasuraman, T.M. Lim, C. Menictas, M. Skyllas-Kazacos, Electrochim. Acta 101 (2013) 27–40.
[8] M. Park, J. Ryu, J. Cho, Chem. – Asian J. 10 (2015) 2096–2110.
[9] L. Thi Xuan Huong, M. Bechelany, M. Cretin, Carbon 122 (2017) 564–591.
[10] K.J. Kim, M.-S. Park, Y.-J. Kim, J.H. Kim, S.X. Dou, M. Skyllas-Kazacos, J. Mater. Chem. A 3 (2015) 16913–16933.
[11] B.T. Sun, M. Skyllas-Kazacos, Electrochim. Acta 36 (1991) 513–517.
[12] S. Zhong, C. Padeste, M. Kazacos, M. Skyllas-Kazacos, J. Power Sources 45 (1993) 29–41.
[13] B. Sun, M. Sykllaskazacos, Electrochim. Acta 37 (1992) 1253–1260.
[14] B. Sun, M. Skyllas-Kazacos, Electrochim. Acta 37 (1992) 2459–2465.
[15] W.G. Zhang, J.Y. Xi, Z.H. Li, H.P. Zhou, L. Liu, Z.H. Wu, X.P. Qiu, Electrochim. Acta 89 (2013) 429–435.
[16] H. Liu, L. Yang, Q. Xu, C. Yan, RSC Adv. 4 (2014) 55666–55670.
[17] Z. He, Y. Jiang, W. Meng, F. Jiang, H. Zhou, Y. Li, J. Zhu, L. Wang, L. Dai, Appl. Surf. Sci. 423 (2017) 111–118.
[18] C. Gao, N. Wang, S. Peng, S. Liu, Y. Lei, X. Liang, S. Zeng, H. Zi, Electrochim. Acta 88 (2013) 193–202.
[19] J.-Z. Chen, W.-Y. Liao, W.-Y. Hsieh, C.-C. Hsu, Y.-S. Chen, J. Power Sources 274 (2015) 894–898.
[20] D. Dixon, D.J. Babu, J. Langner, M. Bruns, L. Pfaffmann, A. Bhaskar, J.J. Schneider, F. Scheiba, H. Ehrenberg, J. Power Sources 332 (2016) 240–248.
[21] K.J. Kim, Y.J. Kim, J.H. Kim, M.S. Park, Mater. Chem. Phys. 131 (2011) 547–553.
[22] K.J. Kim, S.-W. Lee, T. Yim, J.-G. Kim, J.W. Choi, J.H. Kim, M.-S. Park, Y.-J. Kim, Sci. Rep. 4 (2014).
[23] X. Wu, H. Xu, Y. Shen, P. Xu, L. Lu, J. Fu, H. Zhao, Electrochim. Acta 138 (2014) 264–269.
[24] X. Wu, H. Xu, P. Xu, Y. Shen, L. Lu, J. Shi, J. Fu, H. Zhao, J. Power Sources 263 (2014) 104–109.

[25] A. Di Blasi, O. Di Blasi, N. Briguglio, A.S. Arico, D. Sebastian, M.J. Lazaro, G. Monforte, V. Antonucci, J. Power Sources 227 (2013) 15–23.
[26] L. Estevez, D. Reed, Z. Nie, A.M. Schwarz, M.I. Nandasiri, J.P. Kizewski, W. Wang, E. Thomsen, J. Liu, J.-G. Zhang, V. Sprenkle, B. Li, ChemSusChem 9 (2016) 1455–1461.
[27] Y. Shao, X. Wang, M. Engelhard, C. Wang, S. Dai, J. Liu, Z. Yang, Y. Lin, J. Power Sources 195 (2010) 4375–4379.
[28] J. Jin, X. Fu, Q. Liu, Y. Liu, Z. Wei, K. Niu, J. Zhang, ACS Nano 7 (2013) 4764–4773.
[29] T. Wu, K.L. Huang, S.Q. Liu, S.X. Zhuang, D. Fang, S. Li, D. Lu, A.Q. Su, J. Solid State Electr. 16 (2012) 579–585.
[30] Z.X. He, A.Q. Su, C. Gao, Z. Zhou, C.Y. Pan, S.Q. Liu, Ionics 19 (2013) 1021–1026.
[31] H. Lee, H. Kim, J. Appl. Electrochem 43 (2013) 553–557.
[32] Z. He, Z. Chen, W. Meng, Y. Jiang, G. Cheng, L. Dai, L. Wang, J. Energy Chem. 25 (2016) 720–725.
[33] K.J. Kim, H.S. Lee, J. Kim, M.-S. Park, J.H. Kim, Y.-J. Kim, M. Skyllas-Kazacos, ChemSusChem 9 (2016) 1329–1338.
[34] C. Flox, J. Rubio-Garcia, M. Skoumal, T. Andreu, J.R. Morante, Carbon 60 (2013) 280–288.
[35] H.J. Lee, D. Kil, H. Kim, J. Electrochem. Soc. 163 (2016) A2586–A2591.
[36] M.E. Lee, H.-J. Jin, Y.S. Yun, RSC Adv. 7 (2017) 43227–43232.
[37] J. Kim, H. Lim, J.-Y. Jyoung, E.-S. Lee, J.S. Yi, D. Lee, Carbon 111 (2017) 592–601.
[38] C. Li, B. Xie, J. Chen, J. He, Z. He, RSC Adv. 7 (2017) 13184–13190.
[39] J. Kim, H. Lim, J.-Y. Jyoung, E.-S. Lee, J.S. Yi, D. Lee, Electrochim. Acta 245 (2017) 724–733.
[40] J. Ryu, M. Park, J. Cho, J. Electrochem. Soc. 163 (2016) A5144–A5149.
[41] R. Schweiss, J. Power Sources 278 (2015) 308–313.
[42] G. Wei, W. Su, Z. Wei, X. Fan, J. Liu, C. Yan, Electrochim. Acta 204 (2016) 263–269.
[43] G. Wei, W. Su, Z. Wei, M. Jing, X. Fan, J. Liu, C. Yan, Electrochim. Acta 199 (2016) 147–153.
[44] J. Langner, M. Bruns, D. Dixon, A. Nefedov, C. Woell, F. Scheiba, H. Ehrenberg, C. Roth, J. Melke, J. Power Sources 321 (2016) 210–218.
[45] N. Pour, D.G. Kwabi, T. Carney, R.M. Darling, M.L. Perry, Y. Shao-Horn, J. Phys. Chem. C 119 (2015) 5311–5318.
[46] J. Maruyama, S. Maruyama, T. Fukuhara, K. Hanafusa, J. Phys. Chem. C 121 (2017) 24425–24433.
[47] T. Liu, X. Li, C. Xu, H. Zhang, ACS Appl. Mater. Interfaces 9 (2017) 4626–4633.
[48] Y.-C. Chang, J.-Y. Chen, D.M. Kabtamu, G.-Y. Lin, N.-Y. Hsu, Y.-S. Chou, H.-J. Wei, C.-H. Wang, J. Power Sources 364 (2017) 1–8.
[49] D.M. Kabtamu, J.-Y. Chen, Y.-C. Chang, C.-H. Wang, J. Power Sources 341 (2017) 270–279.
[50] Z. Zhang, J. Xi, H. Zhou, X. Qiu, Electrochim. Acta 218 (2016) 15–23.
[51] X.L. Zhou, T.S. Zhao, Y.K. Zeng, L. An, L. Wei, J. Power Sources 329 (2016) 247–254.
[52] L. Dai, Y. Jiang, W. Meng, H. Zhou, L. Wang, Z. He, Appl. Surf. Sci. 401 (2017) 106–113.
[53] Y. Lv, J. Zhang, Z. Lv, C. Wu, Y. Liu, H. Wang, S. Lu, Y. Xiang, Electrochim. Acta 253 (2017) 78–84.
[54] J.J. Park, J.H. Park, O.O. Park, J.H. Yang, Carbon 110 (2016) 17–26.
[55] M. Park, J. Ryu, Y. Kim, J. Cho, Energy Environ. Sci. 7 (2014) 3727–3735.
[56] L. Wei, T.S. Zhao, G. Zhao, L. An, L. Zeng, Appl. Energy 176 (2016) 74–79.
[57] W. Li, J. Liu, C. Yan, Carbon 49 (2011) 3463–3470.
[58] G. Wei, C. Jia, J. Liu, C. Yan, J. Power Sources 220 (2012) 185–192.
[59] W. Li, J. Liu, C. Yan, Electrochim. Acta 79 (2012) 102–108.
[60] S. Wang, X. Zhao, T. Cochell, A. Manthiram, J. Phys. Chem. Lett. 3 (2012) 2164–2167.
[61] J. Friedl, C.M. Bauer, A. Rinaldi, U. Stimming, Carbon 63 (2013) 228–239.
[62] W. Li, J. Liu, C. Yan, J. Solid State Electrochem. 17 (2013) 1369–1376.
[63] M. Steimecke, S. Ruemmler, N.-F. Schuhmacher, T. Lindenberg, M. Hartmann, M. Bron, Electroanalysis 29 (2017) 1056–1061.
[64] G. Wei, J. Liu, H. Zhao, C. Yan, J. Power Sources 241 (2013) 709–717.
[65] G. Wei, M. Jing, X. Fan, J. Liu, C. Yan, J. Power Sources 287 (2015) 81–86.
[66] G. Wei, Z. Gao, Z. Wei, X. Fan, J. Liu, C. Yan, Phys. Chem. Chem. Phys. 17 (2015) 20368–20375.
[67] Z. He, L. Liu, C. Gao, Z. Zhou, X. Liang, Y. Lei, Z. He, S. Liu, RSC Adv. 3 (2013) 19774–19777.
[68] Z. Gonzalez, C. Botas, C. Blanco, R. Santamaria, M. Granda, P. Alvarez, R. Menendez, J. Power Sources 241 (2013) 349–354.
[69] Z. Gonzalez, C. Botas, C. Blanco, R. Santamaria, M. Granda, P. Alvarez, R. Menendez, Nano Energy 2 (2013) 1322–1328.
[70] P. Han, H. Wang, Z. Liu, X. Chen, W. Ma, J. Yao, Y. Zhu, G. Cui, Carbon 49 (2011) 693–700.
[71] X. Rui, M.O. Oo, D.H. Sim, S.C. Raghu, Q. Yan, T.M. Lim, M. Skyllas-Kazacos, Electrochim. Acta 85 (2012) 175–181.
[72] Z. Gonzalez, C. Botas, P. Alvarez, S. Roldan, C. Blanco, R. Santamaria, M. Granda, R. Menendez, Carbon 50 (2012) 828–834.
[73] W. Li, J. Liu, C. Yan, Carbon 55 (2013) 313–320.
[74] M.H. Moghim, R. Eqra, M. Babaiee, M. Zarei-Jelyani, M.M. Loghavi, J. Electroanal. Chem. 789 (2017) 67–75.
[75] L. Shi, S. Liu, Z. He, J. Shen, Electrochim. Acta 138 (2014) 93–100.
[76] M. Park, I.-Y. Jeon, J. Ryu, J.-B. Baek, J. Cho, Adv. Energy Mater. 5 (2015) 1401550.
[77] C. Noh, S. Moon, Y. Chung, Y. Kwon, J. Mater. Chem. A 5 (2017) 21334–21342.
[78] M. Park, I.-Y. Jeon, J. Ryu, H. Jang, J.-B. Back, J. Cho, Nano Energy 26 (2016) 233–240.
[79] P. Han, Y. Yue, Z. Liu, W. Xu, L. Zhang, H. Xu, S. Dong, G. Cui, Energy Environ. Sci. 4 (2011) 4710–4717.
[80] S. Fu, C. Zhu, J. Song, M.H. Engelhard, D. Du, Y. Lin, Electroanalysis 29 (2017) 1469–1473.
[81] M. Park, Y.-J. Jung, J. Kim, H.I. Lee, J. Cho, Nano Lett. 13 (2013) 4833–4839.
[82] W. Li, Z. Zhang, Y. Tang, H. Bian, T.-W. Ng, W. Zhang, C.-S. Lee, Adv. Sci. 3 (2016) 1500276.
[83] Z. Gonzalez, C. Flox, C. Blanco, M. Granda, J.R. Morante, R. Menendez, R. Santamaria, J. Power Sources 338 (2017) 155–162.
[84] D. Aaron, S. Yeom, K.D. Kihm, Y.A. Gandomi, T. Ertugrul, M.M. Mench, J. Power Sources 366 (2017) 241–248.
[85] M.-A. Goulet, A. Habisch, E. Kjeang, Electrochim. Acta 206 (2016) 36–44.
[86] W.H. Wang, X.D. Wang, Electrochim. Acta 52 (2007) 6755–6762.
[87] Z. Gonzalez, A. Sanchez, C. Blanco, M. Granda, R. Menendez, R. Santamaria, Electrochem. Commun. 13 (2011) 1379–1382.
[88] B. Li, M. Gu, Z. Nie, Y. Shao, Q. Luo, X. Wei, X. Li, J. Xiao, C. Wang, V. Sprenlde, W. Wang, Nano Lett. 13 (2013) 1330–1335.
[89] D.J. Suarez, Z. Gonzalez, C. Blanco, M. Granda, R. Menendez, R. Santamaria, ChemSusChem 7 (2014) 914–918.
[90] T. Liu, X. Li, H. Nie, C. Xu, H. Zhang, J. Power Sources 286 (2015) 73–81.
[91] X. Yang, T. Liu, C. Xu, H. Zhang, X. Li, H. Zhang, J. Energy Chem. 26 (2017) 1–7.
[92] X. Wu, H. Xu, L. Lu, H. Zhao, J. Fu, Y. Shen, P. Xu, Y. Dong, J. Power Sources 250 (2014) 274–278.
[93] P. Hien Thi Thu, C. Jo, J. Lee, Y. Kwon, RSC Adv. 6 (2016) 17574–17582.
[94] H. Zhou, J. Xi, Z. Li, Z. Zhang, L. Yu, L. Liu, X. Qiu, L. Chen, RSC Adv. 4 (2014) 61912–61918.
[95] M. Jing, X. Zhang, X. Fan, L. Zhao, J. Liu, C. Yan, Electrochim. Acta 215 (2016) 57–65.
[96] J. Vazquez-Galvan, C. Flox, C. Fabrega, E. Ventosa, A. Parra, T. Andreu, J. Ramon Morante, ChemSusChem 10 (2017) 2089–2098.
[97] C. Yao, H. Zhang, T. Liu, X. Li, Z. Liu, J. Power Sources 218 (2012) 455–461.
[98] Y. Shen, H. Xu, P. Xu, X. Wu, Y. Dong, L. Lu, Electrochim. Acta 132 (2014) 37–41.
[99] H. Zhou, Y. Shen, J. Xi, X. Qiu, L. Chen, ACS Appl. Mater. Interfaces 8 (2016) 15369–15378.
[100] K.J. Kim, M.-S. Park, J.-H. Kim, U. Hwang, N.J. Lee, G. Jeong, Y.-J. Kim, Chem. Commun. 48 (2012) 5455–5457.
[101] Z. He, L. Dai, S. Liu, L. Wang, C. Li, Electrochim. Acta 176 (2015) 1434–1440.
[102] B. Li, M. Gu, Z. Nie, X. Wei, C. Wang, V. Sprenkle, W. Wang, Nano Lett. 14 (2014) 158–165.
[103] C. Yang, H. Wang, S. Lu, C. Wu, Y. Liu, Q. Tan, D. Liang, Y. Xiang, Electrochim. Acta 182 (2015) 834–840.
[104] F.-M. Zhao, G. Wen, L.-Y. Kong, Y.-Q. Chu, C.-A. Ma, Acta Phys.-Chim. Sin. 33 (2017) 1181–1188.
[105] L. Wei, T.S. Zhao, L. Zeng, Y.K. Zeng, H.R. Jiang, J. Power Sources 341 (2017) 318–326.
[106] L. Wei, T. Zhao, L. Zeng, X. Zhou, Y. Zeng, Energy Technol. 4 (2016) 990–996.
[107] A. Ejigu, M. Edwards, D.A. Walsh, ACS Catal. 5 (2015) 7122–7130.
[108] Y. Ji, J.L. Li, S.F.Y. Li, J. Mater. Chem. A 5 (2017) 15154–15166.
[109] T.-M. Tseng, R.-H. Huang, C.-Y. Huang, C.-C. Liu, K.-L. Hsueh, F.-S. Shieu, J. Electrochem. Soc. 161 (2014) A1132–A1138.
[110] P. Han, X. Wang, L. Zhang, T. Wang, J. Yao, C. Huang, L. Gu, G. Cui, RSC Adv. 4 (2014) 20379–20381.
[111] S.-K. Park, J. Shim, J.H. Yang, C.-S. Jin, B.S. Lee, Y.-S. Lee, K.-H. Shin, J.-D. Jeon, Electrochim. Acta 116 (2014) 447–452.
[112] K. Bromberger, J. Kaunert, T. Smolinka, Energy Technol. 2 (2014) 64–76.
[113] T.-C. Chang, J.-P. Zhang, Y.-K. Fuh, J. Power Sources 245 (2014) 66–75.
[114] K. Oh, S. Won, H. Ju, Electrochim. Acta 181 (2015) 13–23.
[115] C.-N. Sun, F.M. Delnick, D.S. Aaron, A.B. Papandrew, M.M. Mench, T.A. Zawodzinski, ECS Electrochem. Lett. 2 (2013) A43–A45.
[116] D.S. Aaron, Q. Liu, Z. Tang, G.M. Grim, A.B. Papandrew, A. Turhan, T.A. Zawodzinski, M.M. Mench, J. Power Sources 206 (2012) 450–453.
[117] Q.H. Liu, G.M. Grim, A.B. Papandrew, A. Turhan, T.A. Zawodzinski, M.M. Mench, J. Electrochem. Soc. 159 (2012) A1246–A1252.
[118] J. Houser, J. Clement, A. Pezeshki, M.M. Mench, J. Power Sources 302 (2016) 369–377.
[119] C. Yao, H. Zhang, T. Liu, X. Li, Z. Liu, J. Power Sources 237 (2013) 19–25.
[120] X.L. Zhou, Y.K. Zeng, X.B. Zhu, L. Wei, T.S. Zhao, J. Power Sources 325 (2016) 329–336.
[121] C. Xu, X. Yang, X. Li, T. Liu, H. Zhang, J. Energy Chem. 26 (2017) 730–737.
[122] X.L. Zhou, T.S. Zhao, L. An, Y.K. Zeng, L. Wei, J. Power Sources 339 (2017) 1–12.
[123] I. Mayrhuber, C.R. Dennison, V. Kalra, E.C. Kumbur, J. Power Sources 260 (2014) 251–258.
[124] A. Bhattarai, N. Wai, R. Schweiss, A. Whitehead, T.M. Lim, H.H. Hng, J. Power Sources 341 (2017) 83–90.
[125] C. Xu, X. Li, T. Liu, H. Zhang, RSC Adv. 7 (2017) 45932–45937.